PRAMANA
— journal of
physics

© Printed in India

Supplement to Vol. 41
December 1993
pp. 55–74

Tests of QCD at LEP

SUNANDA BANERJEE

Tata Institute of Fundamental Research, Bombay 400005, India

Abstract. The four experiments, ALEPH, DELPHI, L3 and OPAL at LEP, have performed a large number of precise measurements to test Quantum Chromodynamics. The strong coupling constant has been measured with high precision : $\alpha_s(M_Z) = 0.123 \pm 0.004$. The coupling constant has been found to be independent of quark flavour. The running of α_s has been demonstrated by the data. Second order QCD matrix element calculations have been tested from several measured distributions in 3-jet and 4-jet events. These distributions give evidence of the vector nature of the gluon and provide measurements of the QCD colour factors. The hadronic distributions are well reproduced by QCD Monte Carlo programs as well as by analytical calculations with soft gluon coherence effects.

1. Introduction

LEP has provided a number of measurements leading to tests of QCD [1-3], the theory of strong interactions. Most of these measurements result from hadronic decays of Z^0. LEP, operating at cm energies near the Z^0 mass, gives rise to large hadronic cross section.This, together with the high luminosity of LEP, leads to large number of events and hence a small statistical error. The four experiments ALEPH [4], DELPHI [5], L3 [6] and OPAL [7], running at LEP, measure events over a large acceptance and with low systematic errors. The high cm energy of LEP leads to better jet resolution and small hadronization correction. The effect of initial state radiation is also small at Z^0. The corrections, being small, give rise to small systematic uncertainties.

The measurments done at LEP to carry out QCD tests can be broadly classified into three categories : (1) the measurement of the strong coupling constant α_s; (2) the testing of the QCD matrix elements; (3) the study of soft gluon coherence effect. In the present review, a short description of QCD and hadronization models is given in section 2. The three types of tests are described in sections 3–5. The results are summarized in section 6.

More complete and detailed reviews can be found in [8,9].

2. QCD and hadronization models

QCD [1-3] is a nonabelian gauge theory of strong interaction between quarks and gluons. This theory is characterized by one parameter, the coupling constant α_s. The coupling constant decreases with energy due to gluon self interaction. For high energies, the coupling constant is sufficiently small (asymtotic freedom [2]), so that perturbative calculations are possible. At low energies (or at short distances), the coupling constant is large leading to colour confinement [10].

The energy dependence of the strong coupling constant is given by the renormalization group equation

$$\mu^2 \frac{\partial \alpha_s}{\partial \mu^2} = -(\beta_0 {\alpha_s}^2 + \beta_1 {\alpha_s}^3 + \beta_2 {\alpha_s}^4 + ...),$$

where μ is the energy scale, and the coefficients β_i's have been calculated [2,11] in terms of number of active flavour N_f,

$$\beta_0 = \frac{1}{4\pi}\left(11 - \frac{2}{3}N_f\right),$$

$$\beta_1 = \frac{1}{(4\pi)^2}\left(102 - \frac{38}{3}N_f\right),$$

$$\beta_2 = \frac{1}{(4\pi)^3}\left(\frac{2857}{2} - \frac{5033}{18}N_f + \frac{325}{54}{N_f}^2\right).$$

In the next to leading order approximation, the renormalization group equation leads to

$$\alpha_s(\mu) = \frac{1}{\beta_0 \ln(\mu^2/\Lambda^2)}\left[1 - \frac{\beta_1}{\beta_0^2}\frac{\ln\ln(\mu^2/\Lambda^2)}{\ln(\mu^2/\Lambda^2)}\right],$$

where Λ is a cutoff parameter indicating the boundary between perturbative and non-perturbative energy ranges. At LEP, one uses the above expression with 5 active flavours and the cross sections are calculated in the $\overline{\mathrm{MS}}$ (modified minimum subtraction) renormalization scheme [12]. These lead to the measurement of $\Lambda^{(5)}_{\overline{\mathrm{MS}}}$.

In LEP experiments, one observes multihadronic final states in e^+e^- collisions. The hadrons are manifested in the form of jets which preserve the energy and direction of the primary partons. Theoretically, hadron production in e^+e^- collisions is visualised as a multistep process [13] : (i) at energy scale $\sim$ 100 GeV, e^+e^- gives rise to a quark-antiquark pair mainly through Z^0 exchange; (ii) the quark-antiquark pair cascades successively through hard gluon emission which can be described by perturbative QCD (upto energy scale of 1–10 GeV); (iii) the partons hadronize to form the stable as well as the unstable hadrons (need nonperturbative calculations); (iv) the unstable particles decay.

The step (ii) is of primary interest here. The perturbative calculation is done either complete to second order (matrix element approach [14]) or to leading log approximation (parton shower approach [15]). The matrix element approach is applicable upto energy scale of 10 GeV and it gives a maximum of 4 partons in the final state. The parton shower approach is carried out to energy scale of $\sim$ 1 GeV and has on average of 9 partons in the final state. In general, the parton shower approach describes the data better. On the other hand, α_s is well defined only in the matrix element approach.

In absence of non-perturbative calculations, the hadronization process needs specific models. There are three different approaches for hadronization : (i) independent fragmentation [16]; (ii) string fragmentation [17]; (iii) cluster fragmentation [18]. There are several Monte Carlo programs available in the market. These

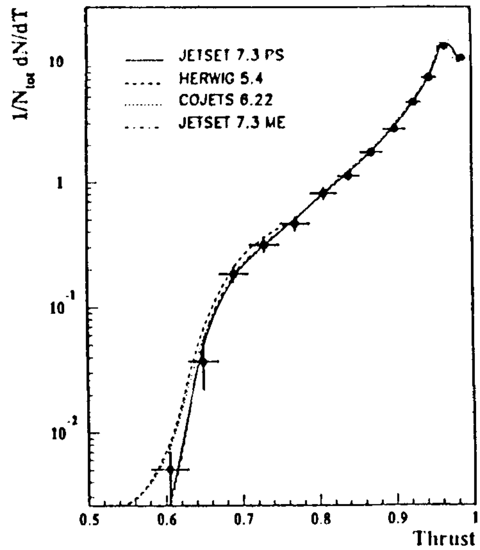

Figure 1. Thrust distribution as measured by L3 in comparison with QCD models.

programs make use of specific choice of perturbative QCD approach and fragmentation models. The particle decays are parametrized from the experimental data available on the unstable particles. Each of these programs JETSET [19], HERWIG [20], ARIADNE [21], NLLJET [22], COJETS [23] comes with a large set of parameters.

The model parameters are tuned so that the models can provide a good description of the experimental data. This is done by choosing (1) only a few critical parameters of the models; (2) distributions of a few global variables which are senistive to these parameters. After tuning, one finds that all the models can describe the data reasonbly well (see Figure 1). The parton shower generators give a better description of the data. Also these models tuned at LEP energies [24-27] can describe low energy e^+e^- data (from PEP, PETRA, TRISTAN) reasonably well.

In all the analyses described in the subsequent sections, the Monte Carlo programs are used to correct the observed distributions from detector effects (resolution and acceptance). The effect of hadronization is applied to the analytical QCD calculations at the time of comparing them to the corrected experimental data.

3. Determination of the strong coupling constant

The strong coupling constant α_s is determined from the hadronic (and also lepton pair) decays of Z^0. The detectors provide energy resolution of $\sim$ 8–10% at $\sqrt{s}$ = 91 GeV for hadronic final states. The charged leptons are measured with momentum resolution of 1–2% at E_{lep} = 46 GeV and jet angular resolution is better than 2.5°. Events are selected and categorised on the basis of global variables like multiplicity, total visible energy, energy imbalance. One achieves a high efficiency (e.g. $\simeq$ 99% for hadrons) in event selection with very low background ($\lesssim$ 0.2%).

3.1. α_s from total cross section

The measurement of the hadronic and leptonic cross sections as a function of cm

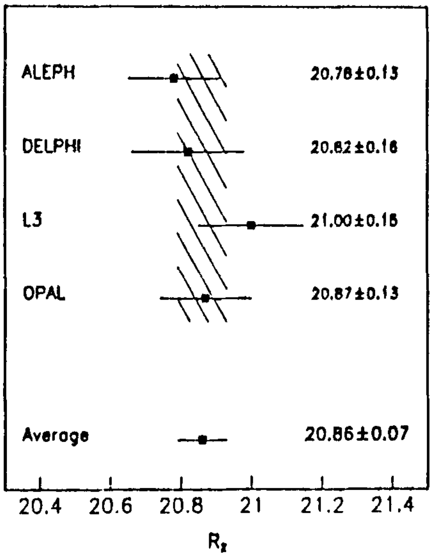

Figure 2. Values of R_Z as measured in the four LEP experiments.

energy leads to the estimation of the partial widths of Z^0 decaying to hadrons and lepton pair. The ratio of the two widths or the peak cross sections (Born term)

$$R_Z \equiv \Gamma_{had}/\Gamma_{lep} \simeq \sigma_0^{had}/\sigma_0^{\ell^+\ell^-}$$

will have small experimental uncertainties (the experimental systematic effects cancel in the ratio). In the Standard Model of electroweak and strong interactions, it is given by

$$R_Z = R_Z^0 \cdot (1 + \delta_{QCD}),$$

where R_Z^0 contains the electroweak coupling constants of quarks and leptons and δ_{QCD} is the QCD correction ($\approx 4\%$). R_Z^0 depends weakly on the top and the Higgs mass values. Using the measured value of M_Z from LEP [28] ($M_Z = 91.187 \pm 0.007$ GeV) and a wide variation of the top and Higgs masses ($m_{top} = 150 \pm 50$ GeV and $M_{Higgs} = 300^{+700}_{-240}$ GeV), one gets

$$R_Z^0 = 19.95 \pm 0.02.$$

The QCD correction can be expressed as [29]

$$\delta_{QCD} = 1.05 \cdot \left(\frac{\alpha_s}{\pi}\right) + 0.9 \cdot \left(\frac{\alpha_s}{\pi}\right)^2 - 13 \cdot \left(\frac{\alpha_s}{\pi}\right)^3,$$

where the third order correction and effect of quark masses have been taken into account.

The LEP data till 1991 (1699K hadronic and 183K leptonic decays of Z^0) have been analysed [28] using the ZFITTER package [30]. The results of this analysis is summarized in Figure 2.

From the average value

$$R_Z = 20.86 \pm 0.07,$$

one gets

$$\alpha_s(M_Z) \;=\; 0.130 \pm 0.011.$$

The uncertainty in the value of α_s is dominated by the experimental uncertainty. The theoretical uncertainty ($\approx 3\%$) is negligible.

In this determination of α_s, some of the α_s sensitive quatities (like the width of Z^0, Γ_Z) are not used. This can be taken care of by performing a simultaneous fit to all the cross sections and asymmetry data with a Standard Model program (also provided by ZFITTER) with four parameters M_Z, m_{top}, M_{Higgs} and α_s. The resulting fit yields

$$\begin{aligned} \alpha_s(M_Z) &= 0.134 \pm 0.009 \pm 0.002, \\ m_{top} &= 134^{+30}_{-38} \pm 18 \text{ GeV}. \end{aligned}$$

The central values of α_s, m_{top} correspond to a Higgs mass value of 300 GeV and the second error corresponds to the range 60 GeV $\leq M_{Higgs} \leq$ 1000 GeV.

3.2. α_s from scaling violation

The normalised momentum distribution is expected to be independent of energy scale in the Quark Parton model. Gluon radiation in QCD introduces a logarithmic energy dependence in the momentum distribution which is termed as scaling violation. The degree of violation is directly related to the strong coupling constant α_s. α_s has been measured from scaling violation in the space-like regime in deep inelastic scattering. In e^+e^- annilations, scaling violation in the fragmentation functions $\overline{D}(x, Q^2)$ can be studied in the time-like region leading to α_s determination.

The fragmentation functions $\overline{D}(x, Q^2)$ are measured from the scaled inclusive momentum distribution

$$\overline{D}(x, Q^2) \equiv \sum_{i=1}^{N_f} W_i(Q^2) D_i(x, Q^2) \equiv \frac{1}{\sigma_{tot}} \frac{d\sigma}{dx}(e^+e^- \to h + X),$$

where $x = p_h/E_b$ (the hadron momentum normalised to the beam energy). $\overline{D}(x, Q^2)$ is the weighted average of the fragmentation functions $D_i(x, Q^2)$ of the individual quark flavours. The weighting functions $W_i(Q^2)$ are determined by the electroweak theory.

The scaling violation is described by the evolution equation [31] which in leading order can be written as

$$Q^2 \frac{\partial}{\partial Q^2} \begin{pmatrix} D_q(x, Q^2) \\ D_g(x, Q^2) \end{pmatrix} = \frac{\alpha_s(Q^2)}{2\pi} \begin{pmatrix} P_{qq} & Pgq \\ 2\sum Pqg & Pgg \end{pmatrix} \otimes \begin{pmatrix} D_q(x, Q^2) \\ D_g(x, Q^2) \end{pmatrix}.$$

The splitting functions $P_{ij}(z)$ are the probabilities of finding the parton i with momentum fraction z from a parton j and can be obtained by integrating the exact QCD matrix element.

An analysis of the LEP data [32] together with low energy data [32,33] from PEP, PETRA, TRISTAN has been carried out. Figure 3 shows Q^2 dependence of the inclusive momentum distribution for various x bins. A fit to these distributions leads to a value of $\alpha_s(M_Z)$ as

$$\alpha_s(M_Z) = 0.119 \pm 0.006.$$

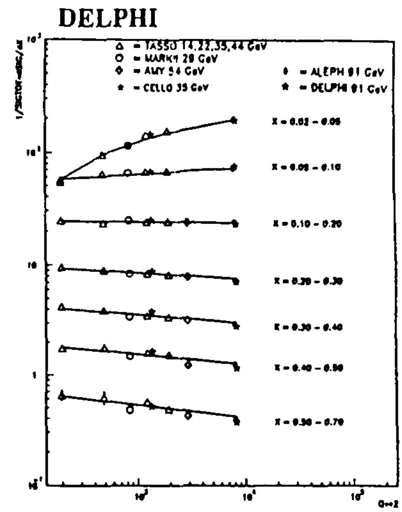

Figure 3. Q^2 dependence of the inclusive momentum spectrum for various x bins.

Table 1. Jet Algorithms

Scheme	y_{ij}	Recombination
JADE [34]	$2E_iE_j(1-\cos\theta_{ij})/s$	$p_k = p_i + p_j$
E_0 [35]	$(p_i+p_j)^2/s$	$E_k = E_i + E_j$; $\vec{p}_k = \frac{E_k}{\lvert\vec{p}_i+\vec{p}_j\rvert}(\vec{p}_i+\vec{p}_j)$
E [35]	$(p_i+p_j)^2/s$	$p_k = p_i + p_j$
p [35]	$(p_i+p_j)^2/s$	$\vec{p}_k = \vec{p}_i + \vec{p}_j$; $E_k = \lvert\vec{p}_k\rvert$
k_T [36]	$2\min(E_i^2, E_j^2)(1-\cos\theta_{ij})/s$	$p_k = p_i + p_j$

The error is dominated by theoretical uncertainty due to uncalculated higher orders.

3.3. α_s from jet multiplicities

Jets are reconstructed out of the observed charged hadrons or calorimetric energy clusters. Most often jet algorithms use a 'distance' variable y_{ij} which determines the closeness of two tracks/clusters i and j. The two tracks/clusters with the smallest y_{ij} are grouped together to form a supercluster k and the four momenta of the particles i,j are combined suitably to give the four momenta of k. The supercluster k then replaces the particles i and j from the list. This procedure is repeated till y_{ij}'s for all combinations of cluster pair exceed a jet resolution parameter y_{cut}. The remaining (super)clusters are called jets. The choice of the 'distance' variable and the recombination scheme has given rise to a variety of algorithms as summarized in Table 1.

The various algorithms differ in (1) their sensitivity to hadronization correction, (2) the possibility of summation to all orders in leading log (or next to leading log) approximation, (3) combining soft particles into jets. For massless partons, the JADE scheme is identical to the E_0 scheme and the hadronization corrections in the two schemes are very similar. Figure 4 shows the hadronization correction factor for various schemes at comparable y_{cut} values (at matching 3-jet fractions). It is clear that JADE and k_T algorithms are the most suitable ones for α_s evaluation.

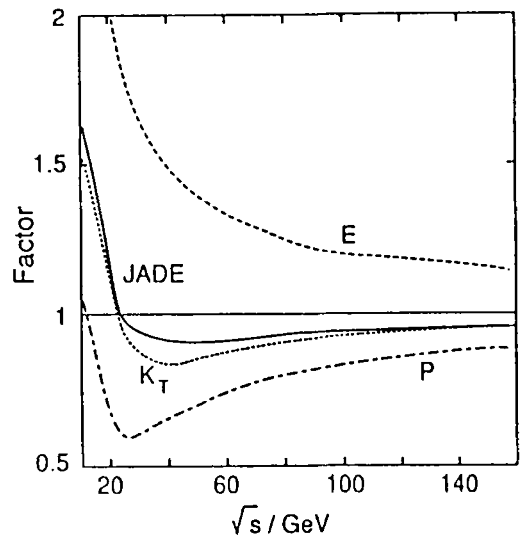

Figure 4. Ratio of 3-jet events after and before hadronization.

As an example, the OPAL [37] analysis is descibed below. OPAL used the JADE algorithm to analyse their hadron data. Jet rates are corrected for detector effects. Second order QCD predicts the rate of 2-, 3- and 4-jet events as a function of $\alpha_s(\mu)$:

$$f_3(y_{cut}) = A_3(y_{cut}) \cdot \alpha_s(\mu) + B_3(y_{cut}, \mu^2/s) \cdot \alpha_s{}^2(\mu),$$
$$f_4(y_{cut}) = B_4(y_{cut}) \cdot \alpha_s{}^2(\mu),$$
$$f_2(y_{cut}) = 1 - f_3(y_{cut}) - f_4(y_{cut}),$$

where μ is the renormalization scale. A_i's and B_i's have been calculated by Kunzst and Nason [35] in the E_0 scheme. The hadronization correction is applied to the theory. The resulting distributions are shown in Figure 5. A fit is performed to the differential distribution $D_2(y)$, which is defined by $(y \equiv y_{cut})$

$$D_2(y) = \frac{f_2(y) - f_2(y - \Delta y)}{\Delta y}.$$

The renormalization scale is chosen using the principle of minimal sensitivity [38], In this principle, the scale μ is chosen from the requirement $(\partial V/\partial f) \equiv 0$ where V is the observable and $f = \mu^2/Q^2$. OPAL measures α_s as

$$\alpha_s(M_Z) = 0.120^{+0.009}_{-0.008}.$$

Simialr measurements exist from ALEPH [39], DELPHI [25], L3 [40], as summarised in Table 2. The error is dominantly due to the uncalculated higher order terms.

3.4. α_s from event shape variables

There exist several global event shape variables like thrust, heavy jet mass, oblateness, C-parameter, etc., which are senisitive to the production of hard gluon jets. Study of these distributions lead to estimates of α_s. Also energy energy correlation and its asymmetry give a measure of α_s. The measurements of α_s from all these variables are highly correlated. On the other hand, the effect of uncalculated

Table 2. α_s measurements from jet rates

Experiment	$\alpha_s(M_Z)$
ALEPH	$0.121 \pm 0.004 \pm 0.007$
DELPHI	$0.112 \pm 0.002 \pm 0.006$
L3	$0.115 \pm 0.005^{+0.012}_{-0.010}$

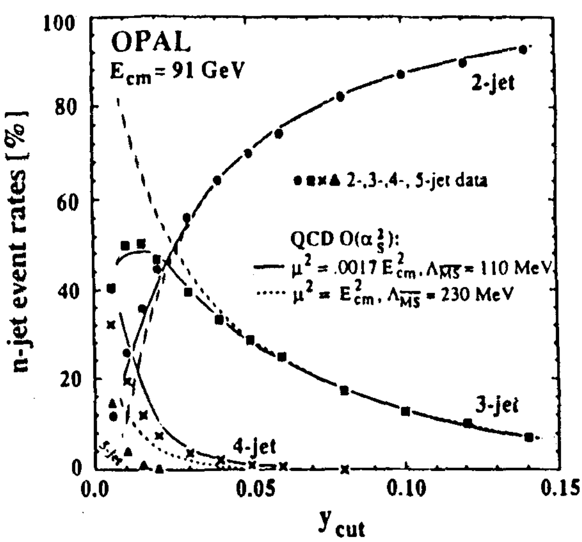

Figure 5. Jet fractions as measured by OPAL.

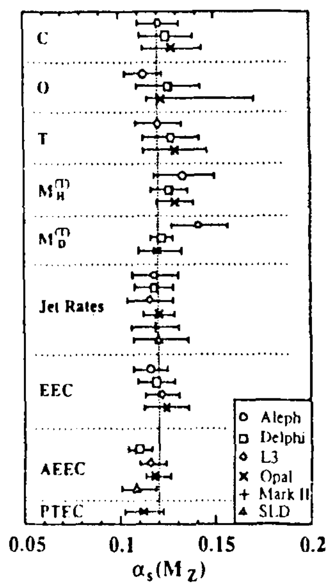

Figure 6. $\alpha_s(M_Z)$ as measured from event shapes, jet rates, energy correlations, in $\mathcal{O}(\alpha_s{}^2)$.

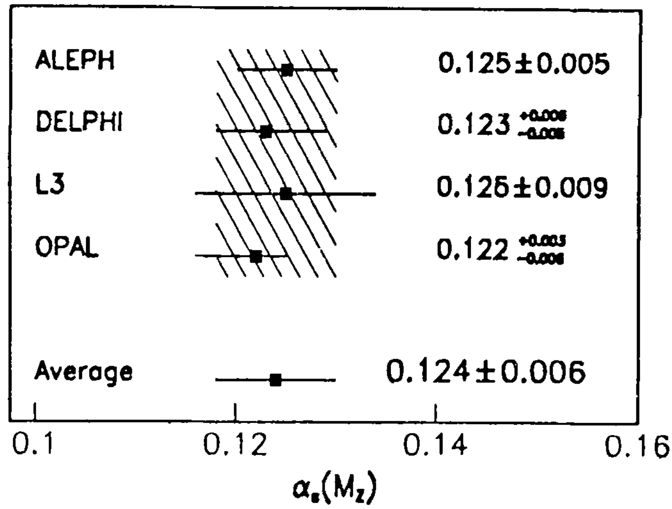

Figure 7. $\alpha_s(M_Z)$ as measued at LEP using resummed $\mathcal{O}(\alpha_s{}^2)$ QCD caculations.

higher order terms are different for these variables. So a careful study, taking care of the correlations, will give a handle to estimate theoretical uncertainty. A consistent analysis combining the results of all the experiments has been performed [9] to complete second order. The results are summarized Figure 6. The unweighted average value from all the experiments gives

$$\alpha_s(M_Z) \;=\; 0.120 \pm 0.006.$$

3.5. α_s from resummed QCD calculations

The QCD predictions in fixed order perturbation theory cannot take into account the effects of multiple gluon emission. This leads to a singular behaviour of the distributions for certain variables in the kinematic regions where multigluon emission is dominant. This is a direct consequence of the colinear and infrared divergences of the gluon emission cross section. It is possible to isolate the single terms in every order of perturbation theory and to sum them up in the form of an exponential. Recently calculations have been carried out which contain, in addition to the complete $\mathcal{O}(\alpha_s{}^2)$ prediction, the resummation of terms of the form $\alpha_s{}^n \ln^m y$ (for observable y) with $m \geq n$. Subleading terms, of the form $\alpha_s{}^n \ln^m y$ with $m < n$, are not included beyond the second order ($n > 2$). Calculations [41] exist for thrust ($y \equiv 1 - T$), heavy jet mass ($y \equiv m_H^2/s$), energy energy correlation ($y \equiv (1 + \cos\chi)/2$) and average jet multiplicity ($y \equiv y_{cut}$).

The resummed calculations are expected to provide more accurate predictions of the distributions, especially in the kinematic regions where multiple gluon emission is dominant. At the same time, they should have a much reduced dependence on the recombination scale compared to the $\mathcal{O}(\alpha_s{}^2)$ calculations. Both these expectations have been confirmed in several recent experimental studies [37,42]. α_s obtained from the four LEP experiments are summarized in Figure 7. The unweighted mean of the four experiments gives

$$\alpha_s(M_Z) \;=\; 0.124 \pm 0.006.$$

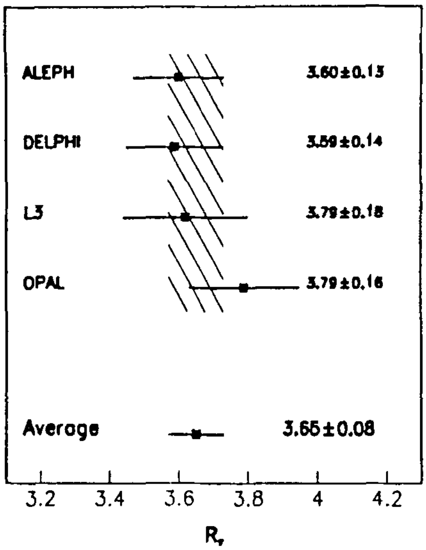

Figure 8. Value of R_τ as measued in the four LEP experiments.

The error is dominated by theoretical uncertainties. The resummed calculations exist for a few observables. More studies are needed to get a better estimate of higher order uncertainties as has been done from the scatter of α_s results from several observables in $\mathcal{O}(\alpha_s{}^2)$ calculations.

3.6. α_s from τ decays

The ratio of hadronic to leptonic partial width of τ has been used to measured the strong coupling constant α_s. The ratio

$$R_\tau \equiv \frac{\Gamma^\tau_{\rm had}}{\Gamma^\tau_{\rm lep}}$$

can be measured independently from the semi leptonic branching ratio of τ and the τ life time. LEP experiments have measured this raio with a high degree of accuracy as seen in Figure 8.

The weighted average of the four measurements is

$$R_\tau^{\rm LEP} = 3.65 \pm 0.08.$$

The inclusive character of the τ hadronic width renders possible an accurate calculation [43] of this ratio using analyticity and operator product expansion. One can write

$$R_\tau = R_\tau^0 \cdot (1 + \delta^\tau_{\rm QCD}),$$

where R_τ^0 contains the CKM matrix elements together with electroweak radiative corrections and nonperturbative contributions. R_τ^0 has been estimated to be

$$R_\tau^0 = 3.028 \pm 0.015.$$

$\delta^\tau_{\rm QCD}$ is the perturbative QCD contribution to R_τ and has been calculated to $\mathcal{O}(\alpha_s{}^3)$ to be

$$\delta^\tau_{\rm QCD} = \left(\frac{\alpha_s(m_\tau)}{\pi}\right) + 5.2 \cdot \left(\frac{\alpha_s(m_\tau)}{\pi}\right)^2 + 26.4 \cdot \left(\frac{\alpha_s(m_\tau)}{\pi}\right)^3.$$

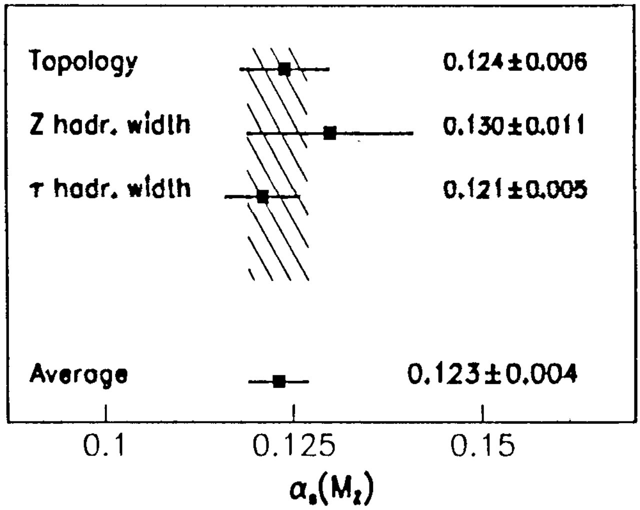

Figure 9. Summary of $\alpha_s(M_Z)$ values measued at LEP.

The LEP measurements give

$$\alpha_s(m_\tau) = 0.36 \pm 0.05$$

and extrapolating to M_Z

$$\alpha_s(M_Z) = 0.121 \pm 0.005.$$

3.7. Summary of α_s results

Figure 9 compares α_s values obtained from R_Z, R_τ and event shape. These three measurements are independent. The measurements from R_Z, R_τ are dominated by experimental uncertainty while that from event shape is dominated by theoretical uncertainty. All these measurements are consistent with each other.

The weighted mean value of

$$\alpha_s(M_Z) = 0.123 \pm 0.004$$

corresponds to

$$\Lambda^{(5)}_{\overline{MS}} = 300 \pm 60 \text{ MeV}.$$

3.8. Running of α_s

α_s has been measured at two energy scales (m_τ and M_Z) from the LEP experiments. The two measurements from the ratio of hadronic to leptonic widths

$$\alpha_s(m_\tau) = 0.36 \pm 0.05,$$
$$\alpha_s(M_Z) = 0.130 \pm 0.011$$

clearly indicate a decrease of α_s with increasing energy. The decrease is a consequence of gluon self-interaction and is one of the most important predictions of QCD.

Figure 10 shows 3-jet fractions observed with the JADE algorithm for $y_{cut} = 0.08$, which have been measured by several experiments at PETRA [34,44],

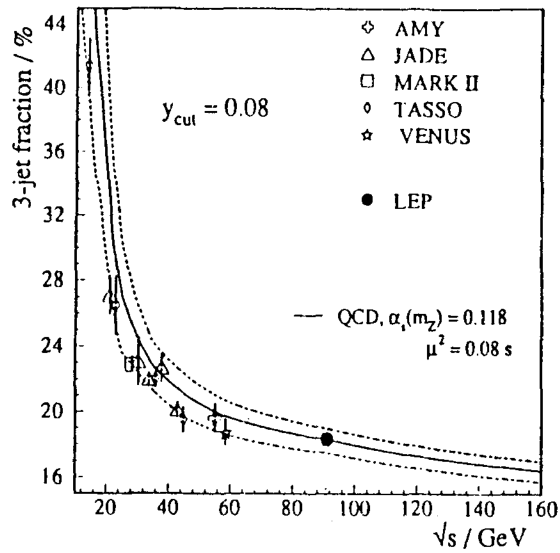

Figure 10. Energy dependence of 3-jet fractions.

PEP [45], TRISTAN [46] and LEP [37,39,40,47]. It is advantageous to compare the measured jet fractions than the coupling constant, since hadronization corrections, matrix element calculations and the renormalization scale used in estimating α_s differ from experiment to experiment. It is clear that the measurements are consistent with QCD calculations with $\Lambda^{(5)}_{\overline{MS}} = 240\,\mathrm{MeV}$ correspoinding to $\alpha_s(M_Z) = 0.118$.

3.9. Flavour dependence of α_s

QCD predicts the coupling constant α_s to be independent of the quark flavour. This has been tested at LEP by studying 3-jet rates in various hadronic samples with tagged primary quark flavour. The L3 collaboration [48] has measured 3-jet rates in two hadronic data sample. The total inclusive sample has 22% $b\bar{b}$ events. The b-quark content has been enhanced in the second sample to 87% by demanding at least one high momentum, high p_T (with respect to the nearest jet) lepton in the event. After corrections for detector, hadronization and b-quark mass effects, one gets the ratio of 3-jet rates for $y_{cut} = 0.05$

$$\frac{f_3^{e,\mu}}{f_3^{had}} = \frac{\sigma^{e,\mu}_{3-jet}}{\sigma^{e,\mu}_{tot}} / \frac{\sigma^{had}_{3-jet}}{\sigma^{had}_{tot}} = 1.00 \pm 0.05,$$

which can be translated into the ratio of α_s values for b-quarks and for u,d,s,c quarks :

$$\frac{{\alpha_s}^{b}}{{\alpha_s}^{u,d,s,c}} = 1.00 \pm 0.08.$$

At PEP/PETRA energies ($\sqrt{s} \approx 30$ GeV), the cross section is proportional to the square of the quark charge (photon exchange). At LEP energies (Z^0 exchange), it is proportional to the sum of the squares of the vector and axial vector coupling constants of the quark. So the flavour composition is different at LEP energy (34% 'up' quark) from that at 30 GeV (73% 'up' quark). Using the 3-jet rates with y_{cut}

= 0.08 and using running of α_s, one gets

$$\frac{\alpha_s^{\mathrm{up}}}{\alpha_s^{\mathrm{down}}} = 0.94 \pm 0.08.$$

These results confirm that α_s is independent of weak isospin or charge of the quark.

4. Test of QCD matrix elements

QCD matrix element calculations have been tested by comparing the measured jet distributions in multijet events to the theoretical predictions. 3-jet events have been used to test the spin-1 of gluon while 4-jet events have been used to test the colour charge of quarks and gluons.

4.1. Three jet events

Jet energy distributions in 3-jet events has been studied by three LEP experiments [49,50]. Jets, reconstructed by the JADE algorithm, are ordered in energy $x_1 \geq x_2 \geq x_3$ where $x_i = 2E_i/\sqrt{s}$. In the lowest order perturbation theory, the cross sections for spin 1 and spin 0 gluons are respectively given by

$$\frac{d\sigma}{dx_q dx_{\bar{q}}} \sim \frac{x_q^2 + x_{\bar{q}}^2}{(1-x_q)(1-x_{\bar{q}})},$$

$$\frac{d\sigma}{dx_q dx_{\bar{q}}} \sim \frac{x_g^2}{(1-x_q)(1-x_{\bar{q}})}.$$

For $x_g \to 0$, the vector gluon cross section becomes large, while it remains small for spin 0 gluons. Figure 11 shows the L3 measurement of x_3 distribution as compared to the spin-1 and spin-0 gluon hypotheses. Experimentally, the x_i's have been determined from jet directions (strictly valid for massless partons), which are measured more precisely than the jet energies. In fact,

$$x_i = \frac{2\sin\psi_i}{\sum_j \sin\psi_j},$$

where ψ_i is the angle between the other two jets excluding the jet i. One sees the data are in excellent agreement with QCD.

The orientation of the three jet event plane with respect to the beam direction has been studied by two LEP experiments [49]. From QCD, one expects the angular distribution to be given by

$$\frac{1}{\sigma}\frac{d\sigma}{d\cos\overline{\Theta}} = \frac{1}{2(1+\overline{\alpha}/3)}(1+\overline{\alpha}\cos^2\overline{\Theta}).$$

In the lowest order QCD, $\overline{\alpha}$ is expected to be $-\frac{1}{3}$ independent of thrust value. Second order corrections are expected to be small. Figure 12 shows $\overline{\alpha}$ plotted as a function of thrust. The data are in excellent agreement with QCD.

The spin-0 model has been ruled out earlier in the PETRA experiments [51]. At LEP, QCD predictions have been tested with a much higher precision.

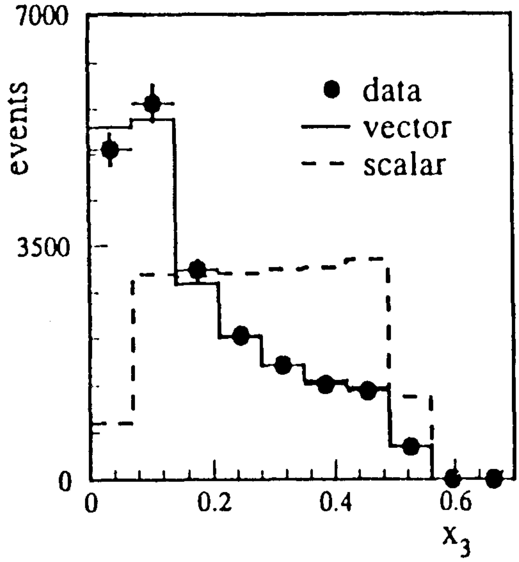

Figure 11. Distribution of energy fraction x_3 as measured by L3.

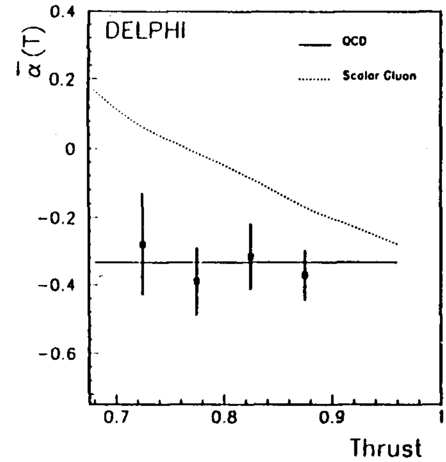

Figure 12. DELPHI measurements of $\overline{\alpha}$ as a function of thrust.

4.2. Four jet events

QCD predicts two classes of 4-jet events at the parton level : $q\bar{q}gg$ (due to double gluon bremsstrahlung and the triple gluon vertex) and $q\bar{q}q\bar{q}$ (from $g \to q\bar{q}$ splitting). The 4-jet differential cross section can be written as

$$\begin{aligned}\sigma_{4-\text{jet}} \sim\ & C_F \cdot \sigma_A + (C_F - C_A/2) \cdot \sigma_B && \text{(double gluon bremsstrahlung)}\\ & + C_A \cdot \sigma_C && \text{(Triple gluon vertex)}\\ & + T_F \cdot N_f \sigma_D + (C_F - C_A/2) \cdot \sigma_E && (q\bar{q}q\bar{q}\ \text{final state}),\end{aligned}$$

where C_A, C_F, T_F are colour factors with values 3, 4/3, 1/2 respectively. If one constructs an abelian model [52] with quarks and gluons, the colour factors get substantially modified (0, 1 and 3 respectively for C_A, C_F, T_F).

The different colour spin structures of the processes $q \to qq$ and $g \to q\bar{q}$ give rise to different predictions of angular correlations within the 4-jet events. DELPHI [53] has studied the double differential distribution of the Nachtmann-Reiter angle [54], $\cos\theta^*_{NR}$ (cosine of the angle between the vectors $\vec{p}_1 - \vec{p}_2$ and $\vec{p}_3 - \vec{p}_4$), and α_{34}, the angle between the two lowest energy jets. θ^*_{NR} discriminates between the $q\bar{q}gg$ and $q\bar{q}q\bar{q}$ final states, whereas α_{34} discriminates between the triple gluon vertex and the double gluon bremsstrahlung terms. ALEPH [55] has carried out an analysis of the five dimensional distribution of jet pair masses, which contains complete information of the 4-jet phase space. Both these analyses determine the ratio of colour factors in a fit to the $\mathcal{O}(\alpha_s{}^2)$ matrix element. The results are summarized in Table 3 together with the expectations of QCD and the abelian model. The results are in good agreement with QCD.

Table 3. Ratio of colour factors

	C_A/C_F	T_F/C_F
DELPHI	2.07 ± 0.31	0.34 ± 0.14
ALEPH	2.24 ± 0.40	0.58 ± 0.29
(QCD)	2.25	0.375
(Abelian)	0.0	3.0

5. Soft gluon coherence effect

Analytical QCD calculations predict gluon interference affecting particle spectra, multiplicities and particle production in between jets.

5.1. Inclusive particle spectra

Inclusive momentum spectra have been calculated [56] in the 'Modified Leading Log Approximation' (MLLA) summing double and single leading-log contributions including the coherence effect. The calculated parton distribution has been directly compared to the measured hadron distribution following 'Local Parton Hadron Duality' [57]. Perturbative QCD predicts a hump-back structure of the inclusive distribution in terms of $\xi_p = \ln(1/x_p)$, where x_p is the normalised particle momentum (with respect to the beam). The peak position is expected to increase with decrease in the particle mass and increase in cm energy.

LEP has measured inclusive particle spectra [58] for several identified hadrons, π^0, η, K^0, Λ and all charged particles. Figure 13a shows the measured ξ_p distributions for π^0, K^0 and all charged particles. The QCD calculations describe the observed distributions rather well. The position of the peak is clearly decreasing with increase in the particle mass as expected in the theory. Figure 13b shows the position of the peak for π^0 and η as a function of centre of mass energy. Again, the QCD calculations reproduce the data rather well.

Thus the MLLA calculations including gluon interference together with the LPHD hypothesis describe the form, energy and particle mass dependence of the inclusive momentum spectra correctly.

5.2. Multiplicities in 3- and 2-jet events

The ratio of the multiplicities of hadrons in the 3- and 2-jet event samples has been recently calculated [59] in the framework of QCD in leading and next to leading log approximation to all orders. The two jet events are due to the fragmentation of two quarks whereas three jet final states are due to one additional gluon jet. So, naively, the ratio of the multiplicities will be related to the net colour charge in each sample, i.e., $(2C_F + C_A)/2C_F$ $(= 17/8)$. However, soft gluon interference will decrease this ratio significantly.

The two LEP experiments [60],L3 and ALEPH, have studied cluster multiplicities in 3- and 2-jet samples with the jets reconstructed using the k_T algorithm. A fixed value of y_{cut} $(\equiv y_1)$ has been chosen to select exclusive three- and two-jet samples. Using the same algorithm but a smaller y_{cut} $(\equiv y_0)$, cluster multiplicities are determined in the two samples. The ratio of the two multiplicities are shown in Figure 14 as a function of y_0.

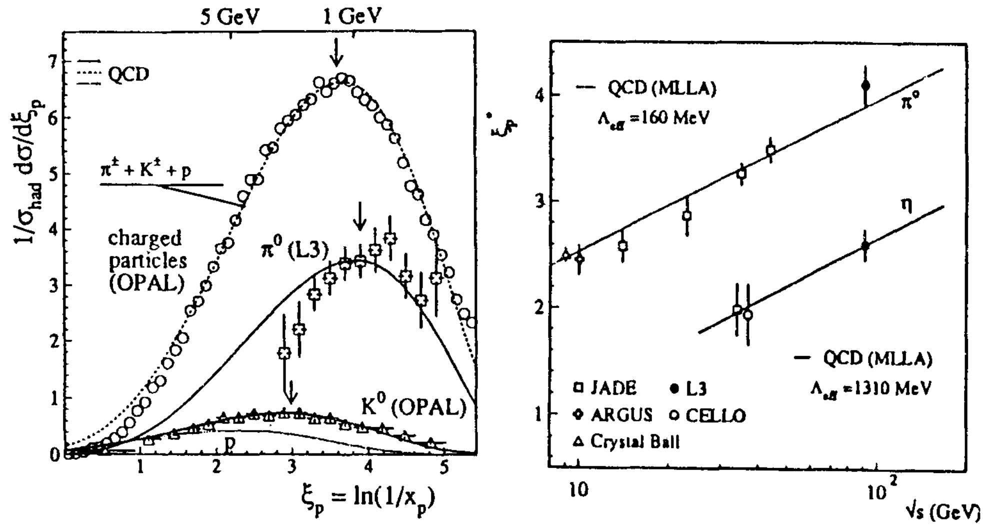

Figure 13. (a) Inclusive ξ_p spectra for π^0, K^0 and charged particles; (b) position of the maximum of ξ_p distributions for π^0 and η.

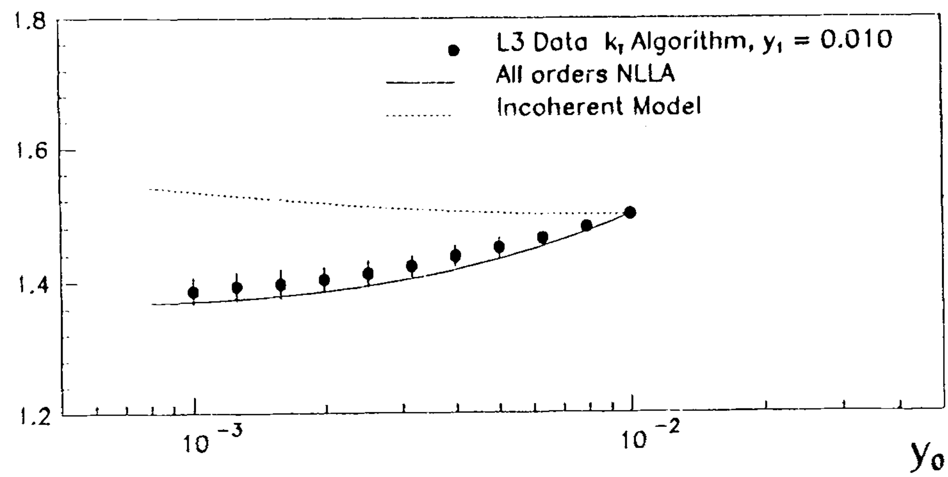

Figure 14. The three jet to two jet cluster multiplicity ratio as measured by L3.

The data are in agreement with the QCD calculations which include the soft gluon interference terms. An 'incoherent' model, where each jet contributes according to its energy without interference, cannot describe the data.

6. Summary

LEP has performed precise measurements of the strong coupling constant. The measurements, obtained using several observables, give a consistent value of α_s. Combining the measurements from event topology, the ratios of hadronic to leptonic widths of Z^0 and τ, one obtains $\alpha_s(M_Z) = 0.123 \pm 0.004$. The coupling constant has been tested to be independent of quark flavour. The energy dependence of α_s has been measured and it is as expected from QCD with $\Lambda^{(5)}_{\overline{MS}} = 240$ MeV.

Many distributions of 3-jet and 4-jet events have been measured with a high degree of accuracy. They can be reproduced by QCD. 3-jet events give evidence of the vector nature of the gluon. 4-jet events provide measurements of QCD colour factors.

String and cluster fragmentation models describe hadronic events quite well. The inclusive momentum spectra of identified hadrons and cluster multiplicities in jets can be described by analytical QCD calculations including soft gluon interference effects.

References

[1] M. Gell-Mann, Acta Physica Austriaca, Suppl. IX (1972) 733;
H. Fritzsch and M. Gell-Mann, Int. Conf. on High Energy Physics, Batavia (1972);
H. Fritzsch *et al.*, Phys. Lett. **47B** (1973) 365.

[2] D.J. Gross and F. Wilczek, Phys. Rev. Lett. **30** (1973) 1343;
D.J. Gross and F. Wilczek, Phys. Rev. **8** (1973) 3633;
H.D. Politzer, Phys. Rev. Lett. **30** (1973) 1346.

[3] G. 't Hooft, Nucl. Phys. **B33** (1971) 173.

[4] ALEPH Collaboration, D. Decamp *et al.*, Nucl. Instrum. Methods **A294** (1990) 121.

[5] DELPHI Collaboration, P. Aarino *et al.*, Nucl. Instrum. Methods **A303** (1991) 233.

[6] L3 Collaboration, B. Adeva *et al.*, Nucl. Instrum. Methods **A289** (1990) 35.

[7] OPAL Collaboration, K. Ahmet *et al.*, Nucl. Instrum. Methods **A305** (1991) 275.

[8] T. Hebbeker, Phys. Reports **217** (1992) 69;
G. Altarelli, talk given at the conference QCD - 20 Years Later, Aachen, June 1992, CERN-TH 6623/92;
S. Bethke, HD-PY 92/12 (1992); HD-PY 92/13 (1992).

[9] S. Bethke and J.E. Pilcher, Ann. Rev. Nucl. Part. Sci. **42** (1992).

[10] S. Weinberg, Phys. Rev. Lett. **31** (1973) 494;
S. Weinberg, Phys. Rev. **D8** (1973) 4482.

[11] W. Caswell, Phys. Rev. Lett. **33** (1974) 244;
D.R.T. Jones, Nucl. Phys. **B75** (1974) 531;
O.V. Tarasov *et al.*, Phys. Lett. **B93** (1980) 429.

[12] G. 'T Hooft, Nucl. Phys. **B61** (1973) 455;
W.A. Bardeen *et al.*, Phys. Rev. **D18** (1978) 3998.

[13] T. Sjöstrand *et al.*,"Z Physics at LEP 1", CERN Report CERN-89-08, Vol.III., p. 143

[14] R.K. Ellis, D.A. Ross and E.A. Terrano, Nucl. Phys. **B178** (1981) 421;
F. Gutbrod, G. Kramer, G. Schierholz, Z. Phys. **C21** (1984) 235.

[15] B.R. Webber, Ann. Rev. Nucl. Part. Sci. **36** (1986) 253.

[16] R.D. Field and R.P. Feynman, Nucl. Phys. **B136** (1978) 1.

[17] B. Andersson *et al.*, Phys. Rep. **97** (1983) 31;
X. Artu, Phys. Rep. **97** (1983) 147.

[18] G.C. Fox and S. Wolfram, Nucl. Phys. **B213** (1983) 65.

[19] T. Sjöstrand, Comput. Phys. Commun. **39** (1986) 347;
T. Sjöstrand and M. Bengtsson, Comput. Phys. Commun. **43** (1987) 367.

[20] G. Marchesini and B.R. Webber, Nucl. Phys. **B310** (1988) 461;
I.G. Knowles, Nucl. Phys. **B310** (1988) 571.

[21] U. Petterson, Lund Preprint LU TP 88-5 (1988);
L. Lönnblad, Lund Preprint LU TP 89-10 (1988), LU TP 91-11 (1991).

[22] K. Kato and T. Munehisa, Phys. Rev. **D39** (1989) 156;
K. Kato and T. Munehisa, Comput. Phys. Commun. **64** (1991) 67.

[23] R. Odorico, Nucl. Phys. **B228** (1983) 381;
R. Odorico, Comput. Phys. Commun. **32** (1984) 139; **34** (1985) 43 (Erratum);
R. Odorico, Comput. Phys. Commun. **59** (1990) 527;
P. Mazzanati and R. Odorico, Nucl. Phys. **B370** (1992) 23.

[24] ALEPH Collaboration, D. Buskulic *et al.*, Z. Phys. **C55** (1992) 209.

[25] DELPHI Collaboration, P. Abreu *et al.*, Z. Phys. **C54** (1992) 55.

[26] L3 Collaboration, B. Adeva *et al.*, Z. Phys. **C55** (1992) 39.

[27] OPAL Collaboration, M.Z. Akrawy *et al.*, Z. Phys. **C47** (1990) 505.

[28] A. Gurtu, talk given at this conference.

[29] T. Hebbeker, Aachen Report PITHA 91/08 (revised).

[30] D. Bardin *et al.*, Nucl. Phys. **B351** (1991) 1;
D. Bardin *et al.*, Z. Phys. **C44** (1989) 493;
D. Bardin *et al.*, Phys. Lett. **B255** (1991) 290;
M. Bilenky and A. Sazonov, JNIR Dubna preprint E2-89-792 (1989) unpublished.

[31] G. Altarelli and G. Parisi, Nucl. Phys. **B126** (1977) 298;
V.N. Gribov and L.N. Lipatov, Sov. J. Nucl. Phys. **15** (1972) 78;
G. Altarelli, Phys. Rep. **81** (1982) 1.

[32] DELPHI Collaboration, W. de Boer *et al.*, DELPHI 92-110 Phys 216, paper submitted to the XXVI International Conference in High Energy Physics, Dallas, August 5-12 1992.

[33] TASSO Collaboration, M. Altoff *et al.*, Z. Phys. **C22** (1984) 307;
TASSO Collaboration, W. Braunschweig *et al.*, Z. Phys. **C47** (1990) 187;
AMY Collaboration, Y.K. Li *et al.*, Phys. Rev. **D41** (1990) 2675;
O. Podobrin, Ph.D. thesis, Univ. of Hamburg, 1992;
MARK-II Collaboration, A. Peterson *et al.*, Phys. Rev. **D37** (1988) 1;
ALEPH Collaboration, D. Decamp *et al.*, CERN PPE/92-62 (1992).

[34] JADE Collaboration, W. Bartel *et al.*, Z. Phys. **C33** (1986) 23;
JADE Collaboration, S. Bethke *et al.*, Phys. Lett. **B213** (1988) 235.

[35] Z. Kunszt and P. Nason in "Z Physics at LEP 1", CERN Report CERN-89-08, Vol.I., p. 373.

[36] Y.L. Dokshitzer, contribution to the Workshop on Jets ar LEP and HERA, Durham (1990);
S. Catani *et al.*, Phys. Lett. **B269** (1991) 432;
N. Brown and W.J. Stirling, Z. Phys. **C53** (1992) 629;
S. Bethke *et al.*, Nucl. Phys. **B370** (1992) 310.

[37] OPAL Collaboration, M.Z. Akrawy *et al.*, Phys. Lett. **B235** (1990) 389.

[38] P.M. Stevenson, Phys. Rev. **D23** (1981) 2916; Nucl. Phys. **B203** (1982) 472; Nucl. Phys. **B231** (1984) 65.

[39] ALEPH Collaboration, D. Decamp *et al.*, Phys. Lett. **B255** (1991) 623.

[40] L3 Collaboration, B. Adeva *et al.*, Phys. Lett. **B248** (1990) 464.

[41] S. Catani *et al.*, Phys. Lett. **B269** (1991) 432;
S. Catani, Proc 17th Workshop on the INFN Eloisatron Project, Erice, June 1991;
S. Catani *et al.*, Phys. Lett. **B263** (1991) 491;
S. Catani *et al.*, Phys. Lett. **B272** (1991) 368;
G. Turncock, Cavendish-HEP-92-3.

[42] ALEPH Collaboration, D. Decamp *et al.*, Phys. Lett. **B284** (1992) 163;
DELPHI Collaboration, H. Fürstenau, QCD - 20 Years Later, Aachen, June 1992;
L3 Collaboration, B. Adeva *et al.*, Phys. Lett. **B284** (1992) 471;
OPAL Collaboration, P.D. Acton *et al.*, Z. Phys. **C55** 1992 1.

[43] E. Braaten, Phys. Rev. Lett. **60** (1988) 1606; Phys. Rev. **D39** (1989) 1458;
S. Narison and A. Pich, Phys. Lett. **B211** (1988) 183;
A. Pich, Proc. Workshop on Tau Lepton Physics, Orsay 1990, 321;
E. Braaten *et al.*, Nucl. Phys. **B373** (1992) 581.

[44] TASSO Collboration, W. Braunschweig *et al.*, Phys. Lett. **B214** (1988) 286.

[45] MARK II Collaboration, S. Bethke *et al.*, Z. Phys. **C43** (1989) 325.

[46] AMY Collaboration, I.H. Park *et al.*, Phys. Rev. Lett. **62** (1989) 1713;
VENUS Collaboration, K. Abe *et al.*, Phys. Lett. **B240** (1990) 232.

[47] DELPHI Collaboration, P. Abreu *et al.*, Phys. Lett. **B247** (1990) 167.

[48] L3 Collaboration, B. Adeva *et al.*, Phys. Lett. **B271** (1991) 461.

[49] DELPHI Collaboration, P. Abreu *et al.*, Phys. Lett. **B274** (1992) 498;
L3 Collaboration, B. Adeva *et al.*, Phys. Lett. **B263** (1991) 551.

[50] OPAL Collaboration, G. Alexander *et al.*, Z. Phys. **C52** (1991) 543.

[51] TASSO Collaboration, R. Brandelik *et al.*, Phys. Lett. **B97** (1980) 453;
PLUTO Collaboration, C. Berger *et al.*, Phys. Lett. **B97** (1980) 459;
CELLO Collaboration, H.J. Behrend *et al.*, Phys. Lett. **B110** (1982) 329;
S.L. Wu, Phys. Rep. **107** (1984) 59.

[52] K.J.F. Gaemers and J.A.M. Vermaseren, Z. Phys. **C7** (1980) 81.

[53] DELPHI Collaboration, P. Abreu *et al.*, Phys. Lett. **B255** (1991) 466.

[54] O. Nachtmann and A. Reiter, Z. Phys. **C16** (1982) 45.

[55] ALEPH Collaboration, D. Decamp *et al.*, Phys. Lett. **B284** (1992) 151.

[56] Y.L. Dokshitzer and S.I. Troyan, Leningrad Preprint LNPI-922 (1984);
Y.I. Azimov *et al.*, Z. Phys. **C27** (1985) 65;
Y.I. Azimov *et al.*, Z. Phys. **C31** (1986) 213;
V.A. Khoze, Y.L. Dokshitzer and S.I. Troyan, Lund Preprint LU TP 90-12.

[57] D. Amati and G. Veneziano, Phys. Lett. **B83** (1979) 87.

[58] ALEPH Collaboration, D. Decamp *et al.*, ALEPH internal note 91-103, July 1991; DELPHI Collaboration, P. Abreu *et al.*, Phys. Lett. **B275** (1992) 231; L3 Collaboration, B. Adeva *et al.*, Phys. Lett. **B259** (1991) 199; L3 Collaboration, O. Adriani *et al.*, Phys. Lett. **B286** (1992) 403; OPAL Collaboration, G. Alexander *et al.*, Phys. Lett. **B264** (1991) 467.

[59] S. Catani *et al.*, Nucl. Phys. **B383** (1992) 419.

[60] L3 Collaboration, contributed paper at XXVI Int. Conf. on High Energy Physics, Dallas, August 1992; ALEPH Collaboration, contributed paper at XXVI Int. Conf. on High Energy Physics, Dallas, August 1992.

Discussion

D. Sankarnarayana : How do you distinguish 4-jet events due to two independently emitted gluons and events which could be attributed to gluon self-coupling ?

S. Banerjee : The two sources of 4-jet events give rise to different distributions in some of the kinematic variables. In particular, the α_{34} distribution in the DELPHI analysis is quite different for double gluon brensstrahlung and for the triple gluon vertex. Global analyses of all kinematic variables give rise to a measure of the various colour factors.

D.P. Roy : Since the energy scale involved in the nonleptonic decay is ~ 1 GeV and it is known to be dominated by the π ρ and A_1 resonences, it may be questionable to estimate α_s from a QCD fit to this process and combine it along with those obtained from Z decay to give an average value.

S, Banerjee : In the exatraction of the α_s from τ-decays, one has to take care of non-pertubative effects. This has been dealt with using analyticity of the spectral functions and the short distance operator product expansion. The method as well as the estimated uncertainty in the non-pertubative calculation is given in the work of E. Braaten et al., Nucl. Phys. **B373** (1992) 581.

R.M. Godbole : How does the measured value of $\alpha_s(M_z)$ from LEP compare with $\alpha_s(M_z)$ measured from DIS measurements?

S. Banerjee : A recent analysis of SLAC/BCDMS gives $\alpha_s(M_z) = 0.113 \pm 0.005$. The average of all the analyses of DIS data leads $\alpha_s(M_z) = 0.111^{+0.004}_{-0.005}$. So these measurements are substantially smaller than the measurements done at LEP. Also quarkonia decays measure $\alpha_s(M_z)$ with small experimental uncertainties. These measurements are also substantially smaller $[\alpha_s(M_z) = 0.113 \pm 0.001\ ^{+0.007}_{-0.005}]$ than the LEP value. Attempts have been made to understand these differences. No concensus has emerged as yet.